REVIEW ARTICLES

Physical Chemical Principles of Photovoltaic Conversion with Nanoparticulate, Mesoporous Dye-Sensitized Solar Cells

Juan Bisquert,*,† David Cahen,*,‡ Gary Hodes,*,‡ Sven Rühle,‡ and Arie Zaban*,§

Departament de Ciències Experimentals, University Jaume 1, 12080 Castelló, Spain, Department of Materials & Interfaces, Weizmann Institute of Science, Rehovot 76100, Israel, and Department of Chemistry, Bar Ilan University, Ramat Gan 52900, Israel

Received: July 4, 2003; In Final Form: December 12, 2003

We review the status of the understanding of dye-sensitized solar cells (DSSC), emphasizing clear physical models with predictive power, and discuss them in terms of the chemical and electrical potential distributions in the device. Before doing so, we place the DSSC in the overall picture of photovoltaic energy converters, reiterating the fundamental common basis of all photovoltaic systems as well as their most important differences.

1. Introduction

Solar energy is one of the most promising future energy resources. The direct conversion of sunlight into electric power by solar cells is of particular interest because it has many advantages over most presently used electrical power generation methods. Electricity is produced without the exhaust of greenhouse gases and without nuclear waste byproducts. The dye-sensitized solar cell (DSSC) appears to have significant potential as a low-cost alternative to conventional p−n junction solar cells. A DSSC consists of a nanocrystalline, mesoporous network of a wide band gap semiconductor (usually TiO_2), which is covered with a monolayer of dye molecules (usually a Ru dye). The semiconductor is deposited onto a transparent conductive oxide (TCO) electrode, through which the cell is illuminated. The TiO_2 pores are filled with a redox electrolyte (I^-/I_3^-) that acts as a conductor and that is electrically connected to a platinum electrode. Upon illumination, electrons are injected from the photoexcited dye into the semiconductor and move toward the TCO substrate, while the electrolyte reduces the oxidized dye and transports the positive charges to the Pt electrode. Such systems can reach solar to electric conversion efficiencies of about 10%[1] but are still not produced on a large scale mainly because of technical problems such as sealing.

At present, p−n junction solar cells are the most efficient light-to-electric power conversion devices, and they are produced in much larger quantities than any other types of solar cell. In a p−n junction solar cell, the difference in the work function between the p and n material leads to a spatial variation of the band energies (reflected in the "bending" of the conduction and valence bands[2]), which is thought to be the main origin of the photovoltaic response. Because of the dominant position of this type of cell, possible alternatives have not attracted very much commercial attention. From a fundamental scientific point of view, most alternatives to the single- or multicrystalline Si cells have often been described in terms of the models that are valid for the latter cell types (i.e., a "diode principle" according to which charge dissociation and charge collection in photovoltaic devices is determined by a built-in electrostatic field). However, this approach should be scrutinized carefully, at least for DSSCs with their nanocrystalline mesoporous electrodes and for most types of organic solar cells.

The photochemical model used to describe photosynthesis is also relevant to the description of DSSC operation.[3,4] In a photochemical converter,[3] light selectively excites the light-absorbing molecules, which constitute part of the converter, and causes a transition of the electronic carriers from a lower, ground level to a higher-lying electronic level. The system can now be viewed as being in a combination of a ground and an excited electronic state. Quasi-chemical potentials of the electrons will be associated with the system in the ground and excited states (by analogy to quasi-Fermi levels or, for brevity, Fermi levels[5]), and their difference determines the amount of useful work (or free energy) that can be obtained as a result of light absorption by such a system. These systems are most often heterogeneous, with different phases microscopically mixed. With the advent of DSSCs and plastic solar cells, some of which are much closer to the photochemical converter than to the photoelectric diode, it became interesting to look for the common denominator of these two seemingly distinct classes of converters to identify their common basic physical features. Recent work has produced useful ideas in this sense, albeit using extremely idealized models.[6−8] Concerning DSSCs, these are questions that have been the subject of discussion and some controversy.[9−13]

The analysis of general principles is scientifically interesting and useful for understanding new kinds of solar cells, even though empirical optimization played a major role in the development of most of today's best cells. Still, there is room for models, with predictive power, that can describe the devices.

* Corresponding authors. E-mail: david.cahen@weizmann.ac.il.
† University Jaume 1.
‡ Weizmann Institute of Science.
§ Bar Ilan University.

10.1021/jp0359283 CCC: $27.50
Published on Web 05/25/2004

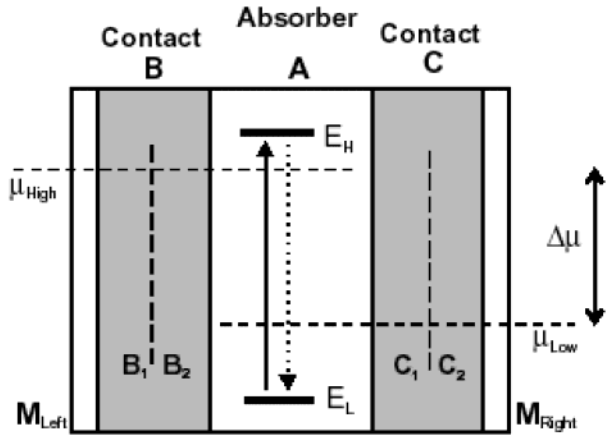

Figure 1. Scheme of an idealized photovoltaic converter. It consists of an absorber, A, in which photon absorption can excite electronic charge carriers, taking the system from a low-energy (L) to a high-energy (H) state with energies E_L and E_H, as indicated by the arrow. Such excitation causes a separation of the chemical potentials of the electrons of the system into μ_{low} and μ_{high}, which reflect the free energy of the electrons in the absorber (i.e., the maximum available free energy[112]). Contacts B and C are selective to electrons having energy equal to or higher than μ_{high} and equal to or lower than μ_{low}, respectively. These contacts maintain the Fermi levels of the two types of carriers from the interface with A up to the outer metal contacts. This model rests on the assumption of completely reversible interfaces for the carriers for the system in state H from A to M_{left} and the complete blockage of carriers for the system in state L by B. Complementary conditions hold for C and H and for L and M_{right}. The only recombination in the cell is the emission process that takes the system from state H to state L, as indicated by the dotted arrow.

These can then lead to design of the optoelectronic properties of the materials, structures and interfaces involved in the system. Therefore, after reviewing some general photovoltaic principles, the remaining parts of this review article will be devoted to the specific aspects of DSSC operation. We will review ideas that have been proposed and models that are thought to describe the DSSC and will discuss them in terms of the chemical (μ) and electrical (ϕ) potential distributions in the device.[115]

2. Photovoltaic Principles

The feature common to all photovoltaic devices including p−n-junction solar cells, photoelectrochemical cells, DSSCs, photogalvanic cells, and organic (plastic) solar cells is the ability to convert solar radiation into electrical power.[14] Very general conditions for photovoltaic action have been indicated in terms of a light-induced change in the work-function difference between the two electrodes,[15] requiring an asymmetry of the circuit.[16]

In general, the process of photovoltaic energy conversion can be divided into two steps:[6,7]

(a) electronic excitation of the absorbing component of the converter by light absorption with concomitant electronic charge creation and

(b) separationof the electronic charges.

The excitation can be an electron−hole pair in a semiconductor, an electronic excitation of a molecule, or the production of excitons. In terms of the two-level system shown in Figure 1, electronic excitation in the absorber promotes the system into a high-energy state, with associated electronic energy level, *H*, simultaneously creating an electron-deficient low-energy state with associated energy level *L*. The electrons in these two states are separated by a difference in enthalpy $\Delta E = E_H - E_L$ (= ($E_C - E_V$) in the case of a semiconductor), and the departure of the populations of the states from their thermal equilibrium values implies a difference in their chemical potential (partial free energy), $\Delta\mu = \mu_H - \mu_L$ ($E_{Fn} - E_{Fp}$, in the case of a semiconductor)[116].

The absorber can be a single molecule, a semiconductor crystal network, or an organic polymer. From the point of view of thermodynamics, the separation of Fermi levels arises as a result of the absorber being at a lower ambient temperature, T_0, than the radiation "pump" temperature, T_p (e.g., the sun).[6] The same conclusion is achieved by treating the absorption−emission process as a chemical equilibrium between the photons and the electronic species in H and L.[17] A Carnot cycle argument[17] or statistical analysis[6] gives the following upper limit for the open-circuit voltage:

$$\Delta\mu = \left(1 - \frac{T_0}{T_p}\right)(E_H - E_L) \qquad (1)$$

To produce electrical output, the photogenerated energy in the absorber must be transferred to the contacts. This can be regarded as the charge-separation step and can be achieved using selective contacts to the absorber. We define an ideally selective contact as one that is transparent to one carrier type and blocks completely the other. In Figure 1, this is shown by $\Delta\mu$ in the absorber promoting a change in the Fermi level (electrochemical potential) of the species in phases B and C with respect to the dark equilibrium situation.

The separation of charges can be effected by a potential gradient. This is the conventional way to view p−n cells where the potential is the electrical potential. As noted recently, the conventional p−n cell can also be viewed in terms of selective contacts if the metal−semiconductor (either n or p) halves of the cell are considered to be such contacts.[8] Because this mechanism of charge separation is more conventional and does not require further explanation, we will concentrate on other mechanisms in the following text.

In the generic scheme of Figure 1, selective electrodes B and C can be treated as filters for each of the carriers (or "valves"[18]), which will enable the two metals, M_{left} and M_{right}, to contact the Fermi levels of the system in the high and low states of the absorber separately at the external leads. The selectivity of contacts to electrons and holes can be achieved via potential barriers at interfaces and by physical layers transparent to only one species. In addition, it can be achieved by details of interfacial charge transfer depending both on kinetic rate constants and on the overlap of the energy levels determining the transfer events. For example, in a DSSC the contact to the dye molecules is selective because of the preferential injection of electrons from the dye in its excited state to the TiO_2 conduction band and hole transfer from the dye ground state to the redox species.

Ideally, B should be reversible to the species in the H state and blocking to the species in the L state. The opposite conditions apply to C. It is important to recognize that a reversible contact to a given species is one that offers no impedance to such species even when current passes.[19]

In Figure 1, metal contacts M are chosen to be of identical composition so that the difference in the Fermi levels in them corresponds to a difference in electric (Galvani) potentials, and under open-circuit conditions, $V_{oc} = \mu_{low} - \mu_{high} = \Delta\mu$ for ideally reversible selective contacts. The change in the Fermi level in phases B and C can be achieved by a modification of the Galvani potential of the phase and/or by a change in the concentration of the species (chemical potential).

TABLE 1: Summary of Photovoltaic Cell Configurations

phenomenon→ ↓type of solar cell↓	light absorbed by[a]	type of mobile charges in device[b]	contact selectivity for charge carriers	current mechanism
p/n junction	semiconductor	electronic	electric field	drift; some diffusion possible
point contact	semiconductor	electronic (+ ionic, for pec variant)[c]	electric field due to contacts	diffusion[c] (electronic charge carriers); diffusion for ions (drift near the contacts)
photogalvanic	dye	ionic	electrochemical kinetics	ion diffusion
photoelectrochemical (PEC)	semiconductor	electronic and ionic	electric field and electrochemical kinetics	ion diffusion and electronic charge carrier drift
nanoporous photoelectrochemical (PEC)	semiconductor	electronic and ionic	electrochemical kinetics	diffusion
organic	semiconductor	electronic (e.g., via excitons)	nature of organic material and/or its interface with the contacts	can be diffusion or drift, depending on cell type
surface-sensitized Schottky barrier	dye	electronic	ballistic, electric field	ballistic and drift
dye-sensitized (DSSC)	dye	electronic and ionic	energy level (mis)match between molecules and semiconductor; electrochemical kinetics	diffusion

[a] Also reflects the nature of high/low energy states; see the text, section 3. [b] In the external circuit, between the metal contacts, these will always be electronic. [c] Contact selectivity is also apparent in the amorphous Si (a-Si:H) p-i-n cells. There, transport is by drift in the i region rather than by diffusion, as in most of the volume of the point contact cell. (See, for example, ref 114.)

Another question of key importance is the structure or geometry of the solar cell. Without aiming at a strict classification, it is useful to distinguish two limiting cases. The first is a configuration in series, where the carrier crossing the entire device will have a single kind of path for doing so. For example, this is the standard geometry of multilayered devices. The second is a heterogeneous configuration, such as in the DSSC or polymer/fullerene blend solar cells.[20] Here, parts of the selective contacts to the absorber, B and C, are closely merged, typically on a scale of nanometers. Thus, a carrier going from M_{right} to M_{left} has distinct paths available for doing so, either by switching several times between B and C or via a percolating path of one of these.

An important drive for investigating heterogeneous devices is the existence of a large internal area where both the excitation in the absorber and charge separation by the selective contacts can be realized. The heterogeneous geometry also improves the collection of incident photons by internal scattering. To these, we can add the low materials cost, ease of fabrication, and low processing temperatures that should permit the preparation of cheap and versatile devices on a large scale. The drawback is that the coexistence of contacts B and C usually reduces their selectivity. Direct recombination between these contacts is a fundamental issue for efficiency and will be reviewed in section 6.

The use of a liquid electrolyte offers a rather effective solution to the problem of electroneutrality in heterogeneous converters. In a compact piece of intrinsic semiconductor, it is not possible to increase the concentration of a single carrier substantially, simply because carriers will repel each other. In contrast, the nanoporous structure of the DSSC permits such an increase, as discussed below, with the assistance of ionic shielding by Li^+ or other cations from a dissolved salt in the liquid phase (which remains highly conducting under all operating conditions of the solar cell).

In the series device based on macroscopic bulk phases (e.g., a p−n junction), the photogenerated electrons and holes are in the same medium. Therefore, these devices rely on crystalline purity, a long lifetime, and the passivation of interfaces (to reduce surface recombination). In the heterogeneous cell, the carriers, which may or may not be generated in the same phase, are rapidly separated into different phases. The very high interfacial area is exploited rather than being seen as a problem. Interfaces are everywhere, so the critical issue is that they should be one-way-only interfaces. This is why the selectivity of contacts is immediately visible in the heterogeneous cells. Because the open-circuit voltage in all solar cells is controlled by recombination (apart from other limiting factors), it is not surprising that the "diode" equation follows both from a series and a heterogeneous mode of operation;[7,21] therefore, the fact that experimental data follow the diode equation is not indicative of any particular cell mode.

3. Photovoltaic Devices

With these questions in mind, we now discuss briefly several kinds of photovoltaic devices, label their high- and low-energy states, point out their transport mechanism, and show in each how the required selectivity at the contacts can be achieved. Thereafter, we will turn our attention to the DSSC. This solar cell gives the best solutions so far to the different problems that need to be solved for the efficient functioning of a heterogeneous converter. Table 1 summarizes the information provided here.

3.1. Point-Contact Solar Cells. These silicon solar cells, developed at Stanford University, are unusual in that both positive and negative contacts are made at the rear surface of the cell. These cells demonstrated 22% efficiency in 1988 and have since been commercialized for operation under concentrated sunlight.[22,23] This configuration provides an almost literal realization of the ideal converter shown in Figure 1 and was also used in a photoelectrochemical configuration to test basic concepts of charge separation.[24−26] The absorber is a thin layer of excellent-quality silicon allowing carrier diffusion lengths that are several times the cell thickness. Photogeneration induces excess carriers in the bulk material and promotes a separation of the Fermi levels of electrons and holes in the sample. Because the absorber silicon layer is only lightly n-doped, the variation in Fermi levels can be attributed to changes in the chemical potentials of the two species (note that there are no "majority" or "minority" carriers in an intrinsic semiconductor) so that the densities of excess carriers are coupled by electroneutrality and transport occurs by ambipolar diffusion. Electrons and holes are separated by electrical potential barriers at point contacts (n^+ and p^+ materials) on one face of the sample. The n^+ and p^+ contacts constitute distinct selective contacts, B and C, to electrons and holes. All of the aspects of the model of Figure 1 were carefully checked by experiment on a PEC configura-

tion:[25] the nearly complete selectivity of the contacts (e.g., the n^+ point transmits electrons with low impedance and rejects holes), the flatness of the Fermi levels throughout the photoconductor, the diode characteristics, and the carrier motion by diffusion by both steady-state and transient transport measurements. The departure from ideality arises from surface recombination.[25]

3.2. Photogalvanic Cells. In the photogalvanic cell, a dye in solution is photoexcited, and the photoexcited chromophore reduces the oxidized form of a redox species in solution. In this solar cell, the solution is the absorber phase, and it is contacted by two metallic electrodes with different selectivity to the redox reaction. Photogalvanic cells have performed only at very low efficiency and stability. Conversion efficiencies of about 0.5% (for 30 min) are typical for the best performance of this type of cell.[27]

3.3. Photoelectrochemical Cell (PEC). The heart of this type of cell is the junction between a semiconductor electrode and a liquid electrolyte. Its mode of action is well described in a manner analogous to that of the basic p−n junction cell with some differences as noted in Table 1.[28]

3.3.a. Porous, Nanoparticulate PEC. Of particular interest to us here is a PEC, made with a porous nanoparticulate semiconductor electrode. In such a photoelectrochemical cell,[29] light is absorbed by the nanoporous semiconductor. Thus, both electrons and holes are present in the semiconductor, in contrast to the case in the DSSC where only one carrier type exists in the semiconductor. Charge-carrier separation is due to kinetic differences in the charge transfer of electrons and holes[30] to the electrolyte. If one charge is more readily injected into the electrolyte, then the other accumulates in the semiconductor and will flow by diffusion to the back contact. Direct electron−hole recombination in the semiconductor is low if the charge transfer to solution is much faster than the direct recombination rate. Recombination can also occur by the injection of the other charge into the electrolyte (the equivalent of back electron transfer from the semiconductor to the electrolyte in the DSSC). Surface states acting as traps may play an important role in this cell by facilitating preferential charge transfer to the solution.[31]

3.4. Organic Cells. Several configurations of solar cells using conjugated polymers (CP) as the light absorber have been studied. We mention first a very simple one that closely follows the principle of Figure 1.[32] It is a three-layer device n-TiO_2/CP/p-CuI where the central polymer absorber is contacted by semiconductor layers selective to electrons (n-TiO_2) and holes (p-CuI). In common with many other CP-based cells, low conversion efficiencies (ca. 0.5%) were obtained. Another configuration that is usually employed is a sandwich of a single organic layer between asymmetric metal contacts, with a low-work-function metal on one side and a high-work-function metal on the opposite side. (For a review, see ref 20.) Cells employing organic semiconductors (OSC) as light absorbers and selective contacts (e.g., n-TiO_2/n-OSC/p-OSC/Au) achieve similar efficiencies.[33]

Power-conversion efficiencies up to ca. 1% have been obtained using two thin (tens of nanometers) organic layers.[34] Often, the open-circuit voltage in this kind of device is attributed to the difference in the work functions of the electrodes, although recent research has shown that the difference in the work functions of the contacts is not the major determining factor for photovoltage in most cases. An investigation of polyfluorene-based bilayer photovoltaic devices found the open-circuit voltage to be much larger than the difference in the electrode work functions (by ∼1 V).[35] Furthermore, a photovoltage of 0.7 V is obtained using symmetric gold metal contacts in the devices.[35] Another study of donor/acceptor porphyrin bilayers interpreted the observed photovoltaic effect in terms of the interfacial kinetics of electron transfer.[9]

Heterogeneous configurations in which the two phases are mixed as interdispersed networks on the nanometer scale have yielded more promising results. In the extensively studied donor (CP)−acceptor (most often a small molecule-like functionalized fullerene) system, light is absorbed by the polymer, and electrons are transferred to the fullerene.[20,36,37] This cell also requires that the heterogeneous layer is sandwiched between two materials with different work functions (e.g., Al, 4.3 eV, and ITO, 4.7 eV).[20] However, V_{oc} is relatively independent of the contact metals and is determined by the energetics of the CP/acceptor pair.[38] To explain these trends, we suggest a simple interpretation of the open-circuit voltage based on the concepts introduced in section 2.

The electron-selective contact to the CP absorber is composed of two materials (ITO, fullerene), which represent B_1 and B_2 in Figure 1. In the first step, the fullerene molecules in the blend accept electrons from the absorber and reject holes; in the second step, the Fermi level of the cathode (e.g., ITO) should equilibrate with the electron Fermi level in the fullerene. Thus, the ITO/fullerene interface should be reversible to electrons. But the CP in the blend is also in contact with the ITO, so the ITO should reject holes. This last effect is facilitated by a layer of poly(3,4-ethylenedioxythiophene) (PEDOT) that is a poor electron conductor and notably improves the selectivity with regard to holes. Thus, the important property of the metal contacts is not their difference in work functions but rather the ability to exchange the electrons reversibly and block the holes and vice versa for the other metal. Of course, a low-work-function metal will favor the former function, and a high one, the latter function. This suggested mechanism of selectivity at the interface also holds for organic−inorganic hybrid devices[39] and is very similar to that of the DSSC.

3.5. Solar Cell with a Single Phase Contact to the Molecular Absorber. A new type of solar cell proposed recently[40] is shown schematically in Figure 2. This cell has a dye/Au/TiO_2 serial structure. Photons incident on the molecular absorber cause the separation of Fermi levels in the TiO_2 and the Au, decreasing the band bending at the Au/TiO_2 space−charge region. But the remarkable point is that the TiO_2 is not in direct contact with the dye, which lies on top of the Au layer. Thus, contact selectivity is achieved with a single material contacting the absorber. The contact to the system in the low-energy state of the absorber (E_L) is the Au layer, where the Fermi level of thermalized electrons communicates with the dye in its electronic ground state. The selective contact to the dye in the high-energy state is obtained by virtue of the Au layer being very thin and allowing the ballistic transfer of electrons to the TiO_2. Therefore, the contact corresponding to B in Figure 1 consists of the combination (Au^H, TiO_2), where the superscript refers to high kinetic energy states in the gold layer. Recombination or decay processes are not shown in Figure 2. A key point for maintaining the selectivity of the contacts is to avoid electron transfer from TiO_2 to Au. A respectable internal quantum efficiency of 10% was reported for this cell.[40]

4. DSSC as a Heterogeneous Converter

The general features of a DSSC are summarized in the schemes of Figure 3, starting with the dark equilibrium situation

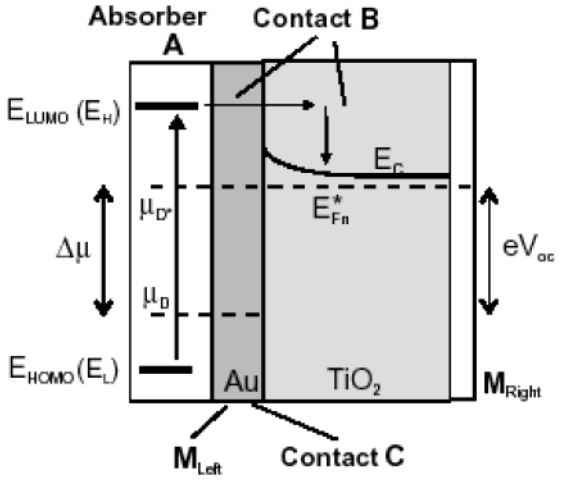

Figure 2. Scheme of a solar cell with a single physical contact to a molecular absorber (merbromin dye)[40] at open circuit. Photons excite the absorber (dye) from a low electronic energy (E_L)[112] to a high electronic energy (E_H) state, as indicated by the arrow. This causes a separation of the chemical potentials of the electrons for the system in the L and H states, where μ_D and μ_D* are the electron chemical potentials of the unexcited and excited dye molecules, respectively.[113] Photoexcited electrons are injected when the dye is in the H state by ballistic transport through the thin Au layer and relax in the TiO_2, as indicated by the small arrow. B and C refer to the selective contacts to the absorber, indicated in Figure 1. The open-circuit voltage is given by $e\Delta\mu$, the difference between the (quasi)Fermi level of conduction-band electrons in TiO_2, by $E^*_{Fn} = \mu_{D^*}$, and that of electrons in the Au layer, by μ_D. M_{left} and M_{right} are as defined in section 2 for Figure 1.

in Figure 3a. Upon illumination (Figure 3b), electrons are injected from the photoexcited dye into the semiconductor and move toward the TCO substrate, while the electrolyte reduces the oxidized dye and transports the positive charges to the Pt electrode. As shown in ref 41, the difference between the electron Fermi level in TiO_2 and the redox potential of the electrolyte, which corresponds to (eV_{OC}), measured between the TCO and the Pt counterelectrode, equals the difference in the electron chemical potentials of the dye in the ground and excited states, $E^*_{Fn} - E_{redox} = \mu_{D^*} - \mu_D$. Figure 3c shows the heterogeneous structure of the DSSC, consisting of two interpenetrating but spatially separated conducting channels. This separation is important for the functioning of selective contacts. As noted above, the contact to the dye in the high-energy state is formed by the TCO-supported TiO_2 layer, and the redox couple forms the selective contact to the dye in the ground state of the dye (Figure 3b). For convenience, these three phases will be denoted α, β, and γ, respectively, as indicated in Figure 3. Because of the small size (about 10 nm) of both of the semiconductor particles and the voids between them, the merged structure represented in Figure 3c allows an enormous increase of electron density in phase β with ionic shielding from phase γ,[42] while providing independent channels for the transport of the respective carriers. Therefore, charge screening can be achieved because of the mesoporous nature of the system.[11,43]

A fundamental step in the transfer of free energy from the dye to the TCO is the increase in the electron chemical potential in the TiO_2 film, resulting from dye injection, as indicated in Figure 3b and also in Figure 4. The essential electrical quantity that relates a change in carrier concentration to a change in potential is the capacitance. Assuming that the TCO/TiO_2 contact is reversible, the local electrochemical potentials of electrons at the contact, $-eV$, and at the Fermi level in the semiconductor network are related simply as $-e\ dV = dE_{Fn}$.[44]

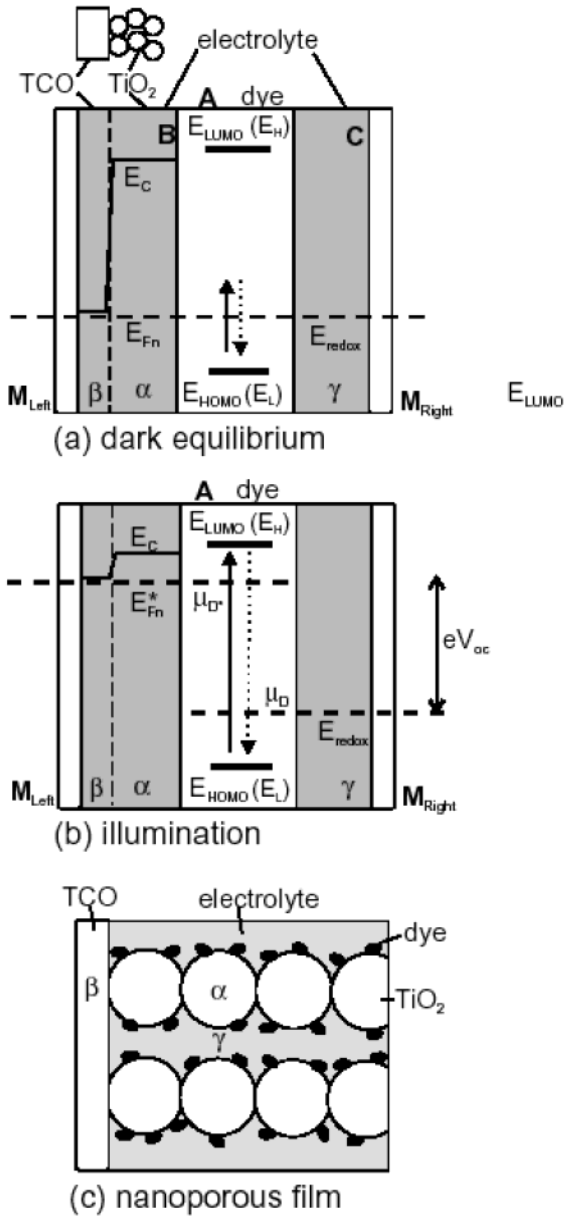

Figure 3. Scheme of a DSSC. (a, b) Selective contacts to the dye molecule (light absorber) in the excited and ground electronic states with energies E_H and E_L.[112] Contact B is formed by a combination of the nanostructured TiO_2 and the TCO. The conduction band (E_c) in these materials is indicated also. Contact C to the low-energy state of the dye is the redox electrolyte. (a) Dark equilibrium situation in which thermal excitation is balanced by radiative emission and the semiconductor Fermi level, E_{Fn}, remains in equilibrium with the redox level in the electrolyte, E_{redox}. (b) Situation under photogeneration at open circuit. μ_D and μ_{D^*} are the chemical potentials of the unexcited and excited dye molecules, respectively.[113] The model assumes completely selective contacts. This means that phase γ can only inject electrons into the dye and phase α can only accept electrons from the dye. Under these conditions, the Fermi level in the semiconductor, E^*_{Fn}, equilibrates to the chemical potential of the excited electrons in the dye, μ_{D^*}. E^*_{Fn} rises above $E_{redox} = \mu_D$ (the change in occupancy of the dye ground state is relatively low), and $-eV_{oc} = \Delta\mu = \mu_{D^*} - \mu_D$, as shown in Figure 1. In reality, if phase γ (electrolyte) accepts electrons from phase α (TiO_2), then the Fermi levels can be straight in both selective contacts, as shown in b, but their difference will be lower than the chemical potential difference in the absorber (dye). If the interface β/α is not completely reversible to electrons, then there will be a drop in the Fermi level toward the TCO. This will also happen if γ accepts electrons from β (TCO). (c) Scheme of the structure of a DSSC showing the spatially separated phases and the dye molecules adsorbed on the surface. The size of particles and voids is typically in the 10-nm range.

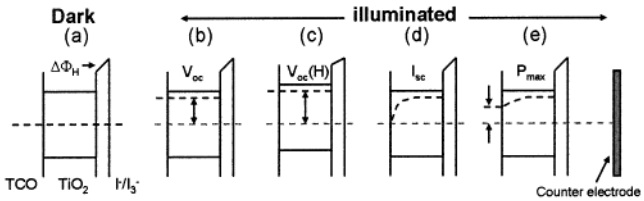

Figure 4. Idealized schemes of the energetics of the DSSC in the dark (a) and upon illumination: at open circuit, V_{oc} (b, c); at short circuit, I_{sc} (d); and at maximum power, P_{max} (e). The schemes emphasize the omnipresence of a potential drop across the Helmholtz layer, $\Delta\Phi_H$, and the effects of possible band-edge shifts due to a change in the Helmholtz potential (cf. double-headed arrows in b and c, which indicate maximum possible photovoltages).

The capacitance per unit volume in the nanoporous film ($C = dQ/dV$) is therefore

$$C = -e\frac{dn}{dV} = e^2\frac{dn}{dE_{Fn}} \tag{2}$$

The density of conduction-band electrons is normally well described by the classical distribution $n = n_0 e^{(E_{Fn}-E_{F0})/k_BT}$, where n_0 is the dark equilibrium value. Assuming that the lower edge of the conduction band does not shift, the variation of the Fermi level in eq 2 corresponds exclusively to the variation of the chemical potential of the electrons. In this case, the capacitance of eq 2 can be termed a chemical capacitance and takes the form

$$C_{ch} = \frac{e^2}{k_BT}n = \frac{e^2}{k_BT}n_0\, e^{(E_{Fn}-E_{F0})/k_BT} \tag{3}$$

Therefore, we can recognize the dominance of the chemical capacitance in the photoelectrode by an exponential dependence of the capacitance on the substrate potential. The different contributions to the capacitance that is actually measured are indicated in Figure 5, as obtained from electrochemical impedance[42,45,46] and cyclic voltammetry.[44] The exponential capacitance is indicated in region B of Figure 5. The chemical capacitance in the DSSC (sometimes called the conduction-band capacitance) can be probed also by electro-optical techniques.[47,48]

Electroneutrality requires that the increase in charge of the particles, due to electrons, will be balanced by a corresponding increase in positive-ion charge at the semiconductor/electrolyte, α/γ interface. Surface charging changes the potential difference across the Helmholtz layer, $\Delta\phi_H$, producing an upward shift of the semiconductor energy levels (cf. Figure 5b and c). Then, the measured capacitance will be given by $C = (C_{ch}^{-1} + C_H^{-1})^{-1}$.

Very often the chemical potential of the electrons dominates the total substrate electrochemical potential in the range of interest. A striking demonstration of this is provided by the correlation of the electronic conductivity with the electrode potential.[49] By combining two experimental techniques, electrochemical impedance spectroscopy (EIS) and the coplanar electrode-gap configuration, the electronic conductivity in nanoporous TiO_2 in aqueous solution can be monitored as a function of the electrode potential. As a result of electron accumulation, the conductivity varies over more than 8 orders of magnitude up to a maximum of $3.7 \times 10^{-3}\ \Omega^{-1}\text{cm}^{-1}$.[49]

Recent impedance measurements of DSSCs have interpreted the above-mentioned exponentially increasing capacitance in terms of junction properties.[50,51] Such an interpretation suggests

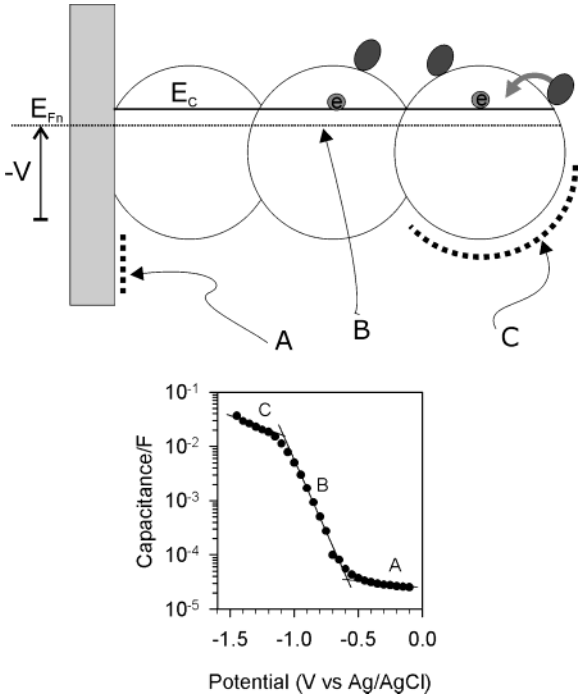

Figure 5. Capacitance (b) of nanostructured TiO_2 in aqueous solution (pH 11) obtained from impedance measurements. The lines are a guide to indicate the domains where different capacitive components are dominant, as indicated in the scheme of a dye-sensitized nanoporous electrode (a). At positive potentials, the TiO_2 matrix is insulating, and the measured capacitance is that of the Helmholtz layer at the interface between the exposed surface of the conducting substrate and the electrolyte (A).[45] At intermediate potentials (B), the electrode potential, V, moves the electron Fermi level, E_{Fn}, with respect to the lower edge of the conduction band, E_c, in the semiconductor nanoparticles. The capacitance is a chemical capacitance due to the increasing chemical potential (activity $\approx$ concentration) of electrons in the TiO_2 phase. At very negative potentials, the semiconductor matrix is electronically conductive, and the constant capacitance at the oxide/electrolyte interface (C) dominates. In C, the capacitance is much larger than in A because of the larger area. In A and C, the energy storage in the capacitor is electrostatic, but in B it is entropic.

that the capacitance that is measured as a diffusion capacitance should be equivalent to an electrostatic capacitor. However, whenever it is possible to separate the electrochemical potential into standard contributions of electrostatic potential (Galvani) energy and chemical potential, there will be both electrostatic and chemical contributions to the capacitance. The chemical capacitance can be defined from thermodynamic considerations.[52,53] It reflects the capability of a system to accept or release additional carriers due to a change in their chemical potential. Energy is stored in the chemical capacitor as a change in entropy.[54] When the chemical capacitance is combined in networks with resistances to describe dissipative processes,[53] transmission lines that are characteristic of diffusion are obtained,[54] as has been shown explicitly for nanostructured semiconductor electrodes.[46,55] However, if diffusive transport is fast, then the diffusion resistance will be small and can be neglected. Then, only the capacitive component and the radiative recombination resistance remain, and these are indeed the necessary elements in the equivalent circuit of a PV converter. Therefore, although any type of solar cell needs a capacitive element,[50] this element need not be an electrostatic one. The chemical capacitor realizes the function of converting excess carriers, induced by light, into an increase of the electrochemical potential of the electrons, which is what ultimately produces the open-circuit voltage.

5. Open-Circuit Voltage in Dye-Sensitized, Mesoporous, Nanoparticulate Cells

We now ask, what is the basic cause of the photovoltage in a DSSC, and which factors determine its limits? To address this question, we first consider the maximum theoretical photovoltage achievable in theory in a perfect DSSC device.

Photon energy is first converted into chemical potential energy in the dye molecules where light absorption occurs, creating an electron−hole pair having a free energy at most that is nearly equal to the dye absorption edge, 1.8 eV for commonly used Ru dyes (cf. eq 1). From this point on, all processes are dissipative and lead to a reduction of the useful (electrical) output energy. Because the actual (rather than the theoretical) open-circuit voltage will ultimately be limited by recombination, it is useful to look for a practical upper limit based on the known energetics of the device.

The most widely used model starts from the assumption that TiO_2 behaves as an intrinsic semiconductor. Charge injection by the dye into such an intrinsic material raises the (quasi)-Fermi level[5] (E_F*) of TiO_2 to close to its conduction-band edge $\{E_F^*(TiO_2) \approx E_C(TiO_2)\}$. Then, assuming that the Fermi level is constant between the TiO_2 particle and the conducting oxide substrate $\{E_F^*(TiO_2) \approx E_C^*(TiO_2)\}$ (see Figure 3b), $E_C(TiO_2)$ is taken as the maximal electrochemical potential of the electron in the electrode. At the same time, the counterelectrode is assumed to take on the potential of the electrolyte (E_{redox}). With both of these assumptions, the model then gives the photovoltage as $E_C(TiO_2) - E_{redox}$.

If many electrons accumulate in the porous TiO_2 structure, then a Helmholtz field will be present at the TiO_2/electrolyte interface (cf. Figure 4), which will shift the band edges, in particular, $E_{CB}(TiO_2)$, with respect to the redox potential. Such a band shift of TiO_2 can proceed in principle up to E_{LUMO}, and the open-circuit voltage, $E_C(TiO_2) - E_{redox}$, gains an additional component by the amount that the TiO_2 band shifts. In principle, at $E_{CB}(TiO_2) = E_{LUMO}$, electron injection from the dye would be suppressed. However, it has been shown[56] that the dye can inject hot (nonthermalized) electrons from (vibronically) excited energy levels above the LUMO, something that will further increase the upper limit to the open-circuit voltage. It was also shown that the redox potential of the dye partially shifts when $E_{CB}(TiO_2)$ moves negatively. (The dye shift depends on the location of the redox center of the dye in the dye layer.[57]) In this case, one may get an even higher open-circuit voltage that is limited by the dye-regeneration process.

The assumption of constant electrochemical potential between the region just outside the Helmholtz layer around the TiO_2 and the counterelectrode is very likely a reasonable one at or near open-circuit conditions (i.e., at low current densities). However, as the current increases, changes will occur in electrolyte composition; therefore, under illumination the assumption may not hold universally. Comparing the average pore size with the thickness of the diffuse layer in the electrolyte provides a simple criterion for this. Namely, as long as the pore size is larger than the diffuse layer thickness there should be no significant potential drop due to a concentration gradient of redox species.

Actually, some potential drop, electrical ($\Delta\phi$) or chemical ($\Delta\mu_e^0$), exists at the TiO_2/TCO interface (but naturally, in electronic equilibrium the electrochemical potential difference will be zero).[43] Indeed, some experimental and theoretical evidence for such a potential drop exists, and it has been suggested that this difference in electrical potential between the conducting oxide and the TiO_2 in the dark is the source of the photovoltage in the DSSC.[11] Because the neutralization of an existing (dark) electric potential difference is involved, this would make this cell similar to a normal p−n junction. However, we have already argued above and have shown with examples that the work-function difference is a criterion that applies to a restricted class of solar cells. In general, the efficient selectivity of contacts can be achieved by electron-transfer kinetics to the materials contacting the light absorber. It would appear that the interpretation of the photovoltage in DSSCs, suggested in ref 11, does not consider the roles of the absorber and the selective contact that we distinguished in section 2. In the DSSC, the cause of photovoltage is the creation of high-energy carriers in the (dye) absorber (where the primary splitting of quasi-Fermi levels is produced), and the selective contact is a necessary condition for obtaining a photovoltage in the outer circuit. The translation of chemical potential to electrostatic potential at the TCO/TiO_2 interface is a key point in the operation in the DSSC (cf. Figure 6), although it is not the origin of photovoltage. Still, the analysis in ref 11 has prompted intensive investigations of this crucial step of the DSSC.[58−61]

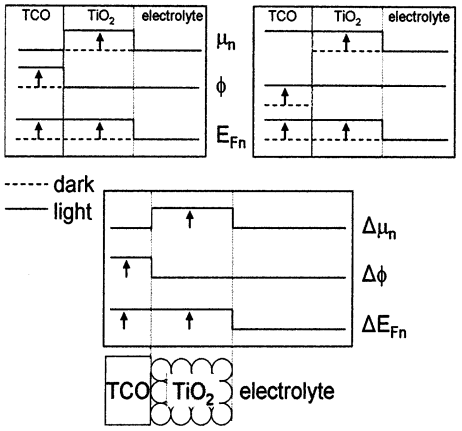

Figure 6. Schematic potential energy diagram of an idealized (1-D) (dye + TiO_2)/TCO/electrolyte system. The top left diagram shows the profiles of the chemical (μ_n), electrostatic (ϕ), and electrochemical (E_{Fn}) potentials for the situation described in ref 51, where an electrostatic potential difference exists in the dark at the TCO/TiO_2 interface. The top right diagram is the same, but in the absence of a built-in electrostatic field at the TCO/TiO_2 interface. The arrows indicate the direction of changes induced by steady-state illumination of the solar cell. The bottom diagram shows where the light-induced changes occur in the chemical ($\Delta\mu_n$), electrostatic ($\Delta\phi$) and electrochemical (ΔE_{Fn}) potential profiles. Note that the bottom diagram relects the changes for BOTH starting situations, that with and the one without the dark electrostatic potential difference at the TCO/TiO_2 interface! In each of the diagrams, each of the potentials has a separate reference level, i.e., they are drawn one under the other for clarity's sake only.

We can now summarize our understanding of the photovoltage generation in a DSSC by looking at how the Fermi level (electrochemical potential of the electrons), the chemical potential of the electrons, and the electrical potential vary across a typical cell structure. This is shown in Figure 6 for the models described here. The Figure shows that, irrespective of the model, the light-induced change in chemical potential of the electrons, which leads to the electrochemical potential shift at the electrolyte/TiO_2 interface, is converted into the change in electrostatic potential at the TiO_2/TCO interface.

6. Recombination

Recombination in DSSCs relates to the reaction of the photoinjected electrons, located in the electron-selective material contacting the dye (the TiO_2), with electron acceptors such as oxidized ions and electron scavengers, located in the hole-

selective phase (electrolyte) or the oxidized dye molecules at the interface between the two phases. These processes decrease the cell performance by affecting all cell parameters (i.e., open-circuit voltage (V_{oc}), short-circuit current (J_{sc}), and fill factor (FF)). The effect of recombination on V_{oc} is often discussed in terms of relative rates (photoinjection versus recombination) or the lifetime of the photoinjected electron in the nanoporous network. The way the short-circuit current is affected by recombination is described in terms of diffusion length or collection efficiency. Between these two extremes, the influence of recombination on the FF integrates the various processes that affect the potential-dependent recombination rate.

The following discussion on recombination in DSSCs will first relate to the microscopic details of this process. Two main issues are considered: First, the electrochemical behavior of the nanoporous semiconductor electrode and the redox mechanism of the electron acceptors (mainly I^-/I_3^- because this redox electrolyte and close derivatives are presently the only efficient ones for DSSCs). In the second part, we will discuss macroscopic behavior with the understanding that the recombination parameters across the cell are not uniform. Finally, we review methods, both those that have been used and possible future ones, to reduce the recombination rate.

6.1. Microscopic Details of Recombination. Three electron acceptors can participate in the recombination process: the oxidized dye molecules, oxidized electrolyte species, and electron scavenger contaminants in the system. The latter may be relevant to the initial operation of the cell, after which they will be fully consumed, unless the electrochemical reaction is fully reversible. No effect on the cell is expected because of the large redox ion concentration. Recombination involving the oxidized dye has been studied extensively and was found to be much slower than the regeneration of the dye by the iodide ion, provided that the ion concentration is higher than 30 mM.[62−65] Because the iodide concentration in standard DSSC electrolytes is much higher than this (typically 500 mM), the primary recombination loss mechanism is between those of the injected electrons and the oxidized ions in solution.

The I^-/I_3^- couple provides two electron acceptors: I_3^- and I_2^-. The rate of recombination with each of these species depends on their concentration (i.e., rate $\propto$ [oxidized ion]^x with reaction orders (x) that probably exceed 1).[47,66] Recently, it was shown that the recombination path depends on the illumination intensity.[67] The electron reaction with I_2^- becomes kinetically favorable only at high light intensities (high injection rates). Under normal solar conditions, the recombination with I_3^- dominates, which makes it the only relevant process from a practical point of view.[67,68]

Since the early days of DSSCs, it was clear that recombination in this system does not obey the simple diode equation. A correlation between the open-circuit voltage and the logarithm of the illumination intensity does not provide a simple linear relation, and the slopes are approximately half of the expected value. In addition, various independent techniques such as intensity-modulated photovoltage spectroscopy (IMVS)[47,66] and open-circuit photovoltage decay[69] reveal a nonlinear dependence of the electron lifetime in TiO_2 electrodes on the electron density. Figure 7 presents the basic uncertainties regarding the electrochemical recombination process of the injected electrons with I_3^- in the solution. For a recombination event to occur, an electron first has to reach the surface of the TiO_2 particle (process A). There is some controversy in the literature regarding the electron distribution in the particles and their transport mechanism.[64,70,71] Several articles have suggested a diffusion-limited recombination mechanism where the electron effects a random walk displacement through the nanoparticle (in some cases, a continuous-time random walk, CTRW) before finding a target recombination site on the surface.[64,71−73] Other approaches emphasize the interfacial events:[70,74] once at the surface, the electron may react through surface states by intermediate trapping events (B), from the conduction-band level (C), or by a combination of the two. The reaction path may also depend on the electron density in the TiO_2. Although the existence of a large number of surface states is commonly accepted, their distribution in the gap is still under discussion. The two possibilities presented in Figure 7, low-energy localized states (D) and an exponential distribution of states toward the conduction-band level (F), were proposed on the basis of electrochemical, photoelectrochemical, and UPS studies.[74,75] Although usually only one possibility is considered, both may coexist.

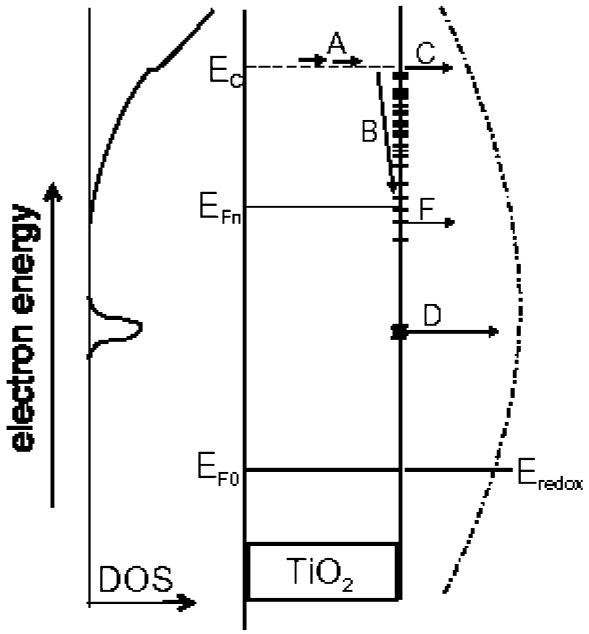

Figure 7. Schematic representation of the steps involved in the recombination between the photoinjected electron and the oxidized species in the electrolyte. E_{F0} shows the position of the Fermi level in the dark, equilibrated with the redox potential (E_{redox}) of the acceptor species in solution. E_{Fn} is the (quasi)Fermi level of electrons under illumination, and E_c is the conduction-band energy. The following steps are indicated: (A) Electron transport; (B) capture by surface states; (C) electron transfer through the conduction band; and (D) deep monoenergetic and (F) exponential distribution of surface states. On the left side, we show the density of electronic states in the TiO_2 nanoparticles, and on the right side, the fluctuating energy levels of oxidized species in solution according to the Marcus−Gerischer model.

The path of the recombination reaction affects the recombination kinetics with respect to two issues, viz., the relevant electron density in TiO_2 and the coupling of the electrons with the electrolyte acceptor states, which can alter the reaction rate by orders of magnitude. (The density of the electrolyte acceptor states is presented qualitatively in Figure 7, right.) In the presence of surface states, as the Fermi level shifts negatively toward the conduction band, the increase in the recombination rate will reflect the intragap surface states' distribution. When an exponential distribution is assumed (Figure 7, left), the rate changes by a power law. Recent measurements[70] support a picture of localized states in the gap (D in Figure 7). In this case, once the states are filled, recombination reaches a maximum rate at relatively low illumination intensities, after

which a steep rise in V_{oc} will result from any increase in the injection rate. In standard DSSCs, the sharp V_{oc} increase occurs around 200 mV,[66] lasting for several tens of millivolts before the recombination rate increases again, showing a dependence on the V_{oc} value (Salvador, P., private communication). One may attribute this last effect to recombination via the conduction band (process C in Figure 7) or to a negative shift of the TiO_2 bands due to the charging of the system (i.e., unpinning of the recombination level[46]). The latter may describe the V_{oc} limit, which seems to be independent of the electrolyte potential.[76,77] In other words, V_{oc} may be limited by the shift of the recombination level into a range of energies that allow "high coupling" with the redox electrolyte, where coupling is the product of the rate constant and the concentration of acceptors near the surface. We note that the distribution of redox states with respect to the redox potential (the DSSC reference) is approximately similar for all organic electrolytes.

6.2. Macroscopic Picture. The macroscopic picture of the recombination process(es) has not yet been deciphered. The system contains at least two electrode materials, TiO_2 and TCO (Figure 3), the charge injection is not uniform through the film, and finally, the electrolyte concentration that depends on the local injection rate and the diffusion to the counterelectrode can vary across the film. At this point, there are not enough data on the ion concentration across the film, which makes it difficult to obtain a clearer picture. However, it is commonly accepted that exposed TCO is a more efficient recombination center ($\beta \rightarrow \gamma$ in Figure 3) than TiO_2. Indeed, recently it was shown that recombination at the TCO and at the first TiO_2 layers near the TCO is faster than that at the rest of the TiO_2 film, generating a constant current flow under open-circuit conditions.[61] Other studies show that blocking of the substrate increases the cell performance.[33,78] However, several issues need to be better clarified, viz., the role of TCO in recombination and the relevant TiO_2 parameters under operating conditions.

6.3. Methods to Reduce the Recombination Rate. The effort to minimize recombination is aimed at two regions of the nanoporous electrode: the high-surface-area nanoporous film and the uncovered area of the conductive substrate (i.e., electron-transfer steps $\alpha \rightarrow \gamma$ and $\beta \rightarrow \gamma$, respectively, in Figure 3c). In principle, these transfer reactions can be suppressed completely, according to the analysis given in section 2.

The high surface area of the semiconductor (α in Figure 3) enhances recombination there. At the conductive substrate (β in Figure 3) recombination depends on the electrocatalytic activity of the TCO to any electron acceptor (in practice, I_3^-) in solution. To minimize this recombination, the electrocatalytic activity should be as low as possible. There are two strategies to reduce this activity. In one, the TCO is coated with a thin compact layer of the same material as that used for the nanoporous film. This film normally has lower electrocatalytic activity towards I_3^- reduction than the TCO. Because the blocking material is an intrinsic or n-type semiconductor, it will block increasingly less effectively as the electrode potential shifts negatively towards V_{oc} due to electron accumulation in this layer. In the other approach, blocking materials such as polyphenoxide are electrodeposited selectively in the areas of the substrate exposed to the electrolyte.[33]

The blocking of the semiconductor is complicated by the presence of the dye that must be connected directly to the semiconductor. Here, also, one may distinguish two approaches. The first approach physically blocks the electrode area that is not covered with dye. The second approach involves the formation of an energy gradient that directs the electrons toward the substrate. Physical blocking involves the adsorption of insulating molecules or the polymerization of an insulating layer on the semiconductor surface after dye adsorption. For example, dip coating of 4-tert-buytlpyridine and polymerization of PPO were tested.[33,79] The energy-gradient approach involves composite material nanoporous electrodes in which the two materials differ by their electron affinity[16,80] (i.e., their conduction-band potential[81−84]). This approach requires a specific electrode design that ensures that the electrons will not encounter energy barriers while diffusing to the current collector. The core−shell electrode, consisting of an inner semiconductor matrix coated by a thin shell with a more negative conduction-band potential, ensures the free diffusion of electrons to the current collector. Using these electrodes, one can significantly increase the efficiency of the DSSC via the improvement of all cell parameters.[84,85] In some cases, the improvement of the conversion efficiency is achieved by a negative shift of the conduction-band potential rather than by the formation of an energy barrier,[0] resulting in a significant V_{oc} increase but with no effect on the other parameters.[84,86,87] The core−shell approach has an advantage over other approaches in that it does not interfere with the dye that is adsorbed after electrode preparation.

7. Transport and General Device Modeling

In section 2, we described a basic scheme of a solar cell where two phases separately contact the light absorber, and these phases also realize the efficient transport of electronic species. In reality, the simultaneous transport of several carriers in heterogeneous systems requires the careful consideration of a number of points, especially the coupling of the different carriers by electroneutrality, which places strong constraints on the permitted densities and also on transport rates. This is known from extensive experience with batteries,[88] membranes, and conducting polymers.

The DSSC, in particular, is a multiple carrier device involving the transport of three electroactive species e^-, I^-, I_3^-, which participate in charge-transfer reactions at several interfaces, plus the inert species (counterion) Li^+. The photooxidized dye (D^+) is positively charged but is immobile. Therefore, a total of five different species participate in charge compensation to satisfy local neutrality. Furthermore, the semiconductor network is a highly disordered medium. Electron transport through it is probably not a simple displacement through extended (conduction band) states as in a homogeneous, crystalline semiconductor. It is likely to be affected and even dominated by a large concentration of localized states, either inside (bulk traps) or at the boundaries (surface states) of the nanoparticles, and probably also by interparticle barriers.

To deal with a heterogeneous system of disordered geometry, it is useful to reduce the multidimensional problem to a 1-D one in the direction of the net macroscopic flux of the electroactive species, normal to the outer electrode planes. The averaging volume is taken to be larger than the dimension defining configurational disorder in the system so that the system is treated as an effectively homogeneous one.[12,14,59] It is also important to maintain the distinction between the two phases existing in the system in order to describe separately the electrical (Galvani) potentials in them, ϕ_i, with i = s (solid) or l (liquid).[89] Local charge neutrality is the fundamental requirement that total charge in the averaging volume element equals zero:

$$c_{Li^+} + c_{D^+} - n - c_{I^-} - c_{I_3^-} = 0 \qquad (4)$$

Several types of constraints define the transport model:

−the continuity equations for the different species, locally relating the rates of variation in the concentration of particles and the divergence of their flux;

−the constitutive equations (or transport equations) that relate the macroscopic flux of each species to the corresponding driving force (the gradient of the electrochemical potential);

−substituting the constitutive equation into the continuity equation for each species yields the evolution equations that relate the time and position dependence of the carrier concentration to the external perturbations (such as carrier generation).

Complete formulations of the classical evolution equations for all the species in a DSSC are available.[90,91] These equations must be complemented with boundary conditions describing the fate of each species at the macroscopic boundaries. The simplest conditions are the reflecting (or blocking) boundary condition for an impermeable boundary and the reversible contact, already discussed above in terms of zero impedance and the continuity of the quasi-Fermi level, equivalent to an ohmic contact (to the species in question) that implies no hindrance to crossing the interface.

One consequence of this general framework is that the inert mobile species, the Li^+ in this case, cannot move in a steady-state situation. Indeed, a net flux of Li^+ ions in some direction would imply their indefinite accumulation at the boundary, which is absurd. Although a flux of inert ions cannot exist, an interaction that retards the displacement of electrons, according to the conditions of local shielding, may not be excluded. In this way, ionic mobility can become a limiting factor for electron diffusivity, and in fact the dependence of the electron diffusion coefficient on the electrolyte properties is well documented.[92−94] Otherwise, the diffusion of the oxidized species of the electrolyte to the Pt electrode is not generally thought to limit cell behavior because of the high concentration of I_3^- ions. Commonly used electrolytes contain 0.5 M of the reduced species (usually I^-) and 0.05 M of the oxidized species (I_3^-), where the latter is equivalent to a charge-carrier density of approximately 3×10^{19} cm^{-3}.

We now summarize the macroscopic transport models relevant to DSSCs, distinguishing between those where large-scale electrical fields, $-\partial\phi_{(i,s)}/\partial x$, are assumed to exist and those where this is not thought to be the case. We emphasize that these macroscopic electrical fields appear as a result of excess carriers and current flow in the device (i.e., these fields need not exist in dark equilibrium) and are consistent with local electroneutrality.

7.1. Models with Large-Scale Electrical Fields. One important model, in which ϕ_s and ϕ_l differ at most by a constant value, is characterized by a common macrohomogeneous field, $-\partial\phi/\partial x$, in the two phases. The problem of this approach in a system with many (>2) species, such as the DSSC, is that the equations are cumbersome and only numerical solutions are possible. This model is well known in a simpler variant for two oppositely charged carriers, known as ambipolar diffusion. In ambipolar diffusion, electroneutrality is expressed as $n = p$, where p is the concentration of holes. The nonequilibrium electrical field $-\partial\phi/\partial x$ builds up between moving carriers to accelerate the slow species and slow the faster one, ensuring that carriers of opposite sign move at the same velocity so that no space charge will develop. However, the comparison of the correct formulation of quasi-neutrality in the DSSC (eq 4) to the electroneutrality condition ($n = p$) indicates that this model is just an empirical or first-order approximation for DSSCs.[94,95] Actually, an important reason for the success of the DSSC is that it is not subject to the condition $n = p$ because of shielding by the highly mobile ionic species in the electrolyte. In heterogeneous solar cells with only two species, the condition $n = p$ may reduce the ambipolar diffusion rate to that of the lowest-mobility species, affecting the efficiency of the device.

In another class of models (as in the classical theory of battery theories and porous electrodes[74,88]), a drift migration force for electrons is due to the macroscopic electrical field in the semiconductor phase, $-\partial\phi_s/\partial x$, related to a position-dependent band shift, $\phi_s(x)$, and ϕ_l = constant. A calculation[13] of the Helmholtz potential in terms of the charging of surface states shows that the resulting driving force increases the diffusion (chemical potential gradient) driving force. However, the analysis given in ref 13 suggests that the effect will be very small.

7.2. Complete Shielding of Electrical Fields in the Two Phases (Electron Diffusion Model). If the spatial variation of $\phi_s(x)$ is neglected, then the external current will be determined by the diffusion of electrons; ionic currents and counterions will locally maintain the continuity of electrical current and quasi-neutrality of charge but need not be explicitly considered. In other words, the transport of the species in high and low Fermi-level phases is essentially decoupled (in macroscopic terms) owing to efficient electrolyte shielding. In two early papers,[29,96] it was suggested that the diffusion of electrons is the dominant transport effect in nanoporous electrodes. Subsequently, an electron diffusion model was formulated,[97] accounting for the photogeneration, transport, and recombination of electrons. An excellent account of the aspects of this model is available.[98]

The electron diffusion model, a single carrier model having the advantage of simplicity, provides a very convenient framework for the discussion of transport features of DSSCs. However, it is clear now that the model as originally formulated[97] is not sufficient to account for the observed features of DSSCs. For instance, a crucial characteristic of any solar cell description is the current−potential curve under illumination. According to the electron diffusion model, the DSSCs can be modeled by a diode equation,[97] given by the sum of a constant photocurrent and a recombination current that equals the dark current (i.e., so-called superposition is valid). Indeed the diode equation can be derived in a much simpler way without having to consider diffusion at all.[7] However, as mentioned before, the simple diode model is known to fail for real DSSCs. At a given potential, the dark current is much smaller than the recombination current under illumination.[99] Furthermore, it was noted that the increase of the current toward the more positive potential is slower than exponential.[100] The diode equation has to be modified by an effective barrier height that depends on the current.[100] Very probably, a fundamental aspect for describing the departure from superposition is to take into account the variation of recombination mechanisms with the electrode potential and the level of illumination, involving different electron-transfer mechanisms through surface states and possible changes in the electrolyte composition.[101]

Although steady-state techniques provide an overall view of DSSC characteristics, another way to obtain detailed information on the physical parameters related to transport and recombination is to use small perturbation techniques at a fixed steady state. Frequency-based techniques such as intensity-modulated photocurrent spectroscopy (IMPS)[102,103] and electrochemical impedance spectroscopy[46,55] have the advantage that frequency-resolved spectra allow the separation of different physicochemical processes. Using the diffusion model in the interpretation of these techniques, it was found that both the effective electron diffusivity, D_n, and the effective electron lifetime, τ_n, that are

measured become a function of the steady state.[47,66,102,104] One is led to assume a variety of electronic states in the nanoporous network, including both extended transport states and localized band-gap states.

Although short-range electron displacement in trap-limited recombination has been described in terms of the CTRW formalism,[71] by far the most widely used approach to long-range electronic motion, involving macroscopic transport equations, is the multiple trapping (MT) model. In this model, diffusive transport through extended states is slowed by (de)-trapping events, and direct hopping between localized states is neglected. Several electrochemical and photoelectrochemical techniques that probe the density of states in nanoporous TiO_2 are consistent with an exponential band tail.[44,75] The mobility decreases rapidly below a certain value of energy E_c defining the transport states so that the motion of a bound electron is limited by the rate of thermal excitations to $E \geq E_c$. MT transport in nanoporous semiconductors and DSSCs has been described by a number of authors.[66,102,105−107]

In the MT model, the effective electron diffusion coefficient D_n that is measured by small perturbation kinetic techniques (interpreted recently as the chemical diffusion coefficient of electrons[108]) contains a factor $(\partial n_L/\partial n_c)$ due to trapping and detrapping events,[109]

$$D_n = \frac{1}{1 + \frac{\partial n_L}{\partial n_c}} D_0 \qquad (5)$$

where D_0 is the diffusion coefficient in the trap-free system, n_c is the density of conduction-band electrons, and n_L is the density of localized electrons in traps. The result in eq 5 (and the simplified expression $D_n = (\partial n_c/\partial n_L)D_0$ for $\partial n_L/\partial n_c \gg 1$) can be derived from the condition of quasi-static equilibrium between free and trapped electrons.[110] The depth of the exponential distribution is characterized by a tailing parameter T_c with units of temperature in the dimensionless coefficient $\alpha = T/T_c$.[48,71] Thus, eq 5 implies a dependence of the type $D_n \propto n_c^{1-\alpha}$.

Concerning the electron lifetime variation with Fermi level (cf. section 6), it was shown[69] that MT implies a similar (but inverse) dependence as in eq 5 for the lifetime $\tau_n = (\partial n_L/\partial n_c)\tau_{n0}$, where τ_{n0} is the free-electron lifetime related to interfacial charge transfer. Therefore, for the case of the exponential distribution of traps, $\tau_n = A n_c^{\alpha-1}\tau_{n0}$, where A is a constant. In this model, the product of D_n and τ_n compensates for the trapping factors $(\partial n_L/\partial n_c)$.[110] Experimentally, a compensation between the lifetime, τ_n, and D_n dependence on incident light intensity has been reported,[66] implying a nearly constant diffusion length for electrons, $L_n = \sqrt{D_n\tau_n}$.

The evidence accumulated so far for a dependence of the effective diffusion coefficient (measured by kinetic techniques) on the Fermi-level position is compelling.[66,102,104−106] As discussed above, the classical MT model provides a simple qualitative explanation for the feature. However, the possibility of an electron-hopping process should not be excluded. The heterogeneous configuration of DSSCs and the variety of possible recombination mechanisms seriously complicate the separation of different effects influencing the experimental results because it is usually not possible to change one parameter without affecting others.

8. Conclusions

Photovoltaic action has been described as the combination of several factors: the creation of excitation by light absorption, charge separation, and extraction of carriers. Selective contacts to the light absorber realize the step of charge separation and in many cases also the function of transporting the electronic species in spatially separated phases that maintain the splitting of Fermi levels obtained at the absorber. The selectivity of contacts to different carriers may be based on potential barriers at interfaces but also on the kinetic conditions of interfacial charge transfer. In the dye-sensitized solar cell, the nanostructured semiconductor is insulating in the dark; the effect of light is to increase the number of electrons in this phase, promoting an increase both of the chemical potential and the electronic conductivity. This chemical potential increase is the key step in the transmission of free energy (photovoltage) between the light absorber (dye) and metal contact. Another important point is the conversion of chemical to electrostatic potential with regard to electrons at the TiO_2/substrate interface. Heterogeneous converters such as dye solar cells have the disadvantage that carriers in the different phases have a large chance of returning from a high to a low Fermi-level phase in a recombination process. Strategies for physically separating the hole- and electron-carrying phases from each other, while permitting the necessary electronic communication through the dye, seem to be a promising route for improving the conversion efficiencies of dye-sensitized nanostructured solar cells.

While this manuscript was being completed, an interesting publication appeared that examines the common properties of dye-sensitized and organic solar cells,[111] with conclusions that are similar to some of ours, especially concerning the kinetic requirements for the selectivity of contacts in heterogeneous solar cells.

Acknowledgment. S.R. thanks the Minerva foundation (Munich) for a predoctoral fellowship. J.B., D.C., and A.Z. thank the Spanish−Israel scientific exchange program for supporting the visits of J.B. and A.Z. D.C. and S.R. thank the EU Research Training Network on "Extremely Thin Absorber (ETA)" solar cells for partial support. J.B. thanks the support Fundació Caixa Castelló under project P1B99-04. A.Z. thanks the support of the Israel Science Foundation. D.C. holds the Shaefer Chair in Energy Research.

References and Notes

(1) O'Regan, B.; Grätzel, M. *Nature* **1991**, *353*, 737.

(2) The bottom of the conduction (top of the valence) band corresponds to the sum of the electron (hole) standard enthalpy and its electrostatic potential.

(3) Ross, R. T. *J. Chem. Phys.* **1966**, *45*, 1−7.

(4) Smestad, G. *Sol. Energy Mater. Sol. Cells* **1994**, *32*, 273−288.

(5) The quasi-Fermi level, also termed "imref" is the nonequilibrium replacement of the Fermi level. Thus, if nonequilibrium instead of equilibrium carrier concentrations are used in the relevant expressions, then the Fermi level has to be replaced by the quasi-Fermi level and vice versa. Different quasi-Fermi levels exist for electrons and holes under nonequilibrium conditions. Following the customary definition of the Fermi energy as the energy that separates the filled from the empty energy levels, no single Fermi level can be defined for intrinsic (and most extrinsic) semiconductors. For further details, see, for example, *Solid State Physics*; Ashcroft, N. W., Mermin, N. D., Eds.; Saunders: Philadelphia, PA, 1976. The redox potential of an electrolyte can be viewed as its "Fermi level" (even though strictly speaking this is an oxymoron because there are no "free" electrons in a redox electrolyte and Fermi−Dirac statistics is applicable only to free electrons) because at 0 K the Fermi level equals the chemical potential of the electron, μ_e. As long as the temperature dependence of μ_e is very small, the two terms can be used interchangeably at finite temperature. For further details, see Reiss, H. *J. Phys. Chem.* **1985**, *89*, 3783.

(6) Landsberg, P. T.; Markvart, T. *Solid-State Electron.* **1998**, *42*, 657−659.

(7) Markvart, T.; Landsberg, P. T. *Physica E* **2002**, *14*, 71−77.
(8) Green, M. A. *Physica E* **2002**, *14*, 11−17.
(9) Savenije, T. J.; Koehorst, R. B. M.; Schaafsma, T. J. *Chem. Phys. Lett.* **1995**, *244*, 363.
(10) Smestad, G.; Bignozzi, C.; Argazzi, R. *Sol. Energy Mater. Sol. Cells* **1994**, *32*, 259.
(11) Schwarzburg, K.; Willig, F. *J. Phys. Chem. B* **1999**, *28*, 5743−5746.
(12) Cahen, D.; Hodes, G.; Grätzel, M.; Guillemoles, J. F.; Riess, I. *J. Phys. Chem. B* **2000**, *104*, 2053−2059.
(13) Vanmaekelbergh, D.; de Jongh, P. E. *J. Phys. Chem. B* **1999**, *103*, 747−750.
(14) Cahen, D.; Grätzel, M.; Guillemoles, J.-F.; Hodes, G. Dye-Sensitized Solar Cells: Principles of Operation. In *Electrochemistry of Nanomaterials*; Hodes, G., Ed.; Wiley-VCH: Weinheim, Germany, 2001; pp 201−228.
(15) Pankove, J. L. *Optical Processes in Semiconductors*; Dover: New York, 1971.
(16) Tauc, J. *Rev. Mod. Phys.* **1957**, *29*, 308.
(17) Ries, H.; McEvoy, A. J. *J. Photochem. Photobiol., A* **1991**, *59*, 11−18
(18) Fonash, S. J. *Solar Cell Device Physics*; Academic: Belton, TX, 1981.
(19) Riess, I.; Schoonman, J. Electrodics. In *CRC Handbook on Solid State Electrochemistry*; Gellings, P. J., Bouwmeester, H. J. M., Eds.; CRC Press: Boca Raton, FL, 1997; p 269.
(20) Brabec, C. J.; Sariciftci, N. S.; Hummelen, J. C. *Adv. Mater.* **2001**, *11*, 15−26.
(21) Shockley, W.; Queisser, H. J. *J. Appl. Phys.* **1961**, *32*, 510.
(22) Cuevas, A.; Sinton, R. A.; Midkiff, N. E.; Swanson, R. M. *IEEE Electron Device Lett.* **1990**, *11*, 6−8 and refs therein.
(23) Green, M. A. Crystalline Silicon Solar Cells. In *Clean Electricity from Photovoltaics*; Archer, M. D., Hill, R., Eds.; Imperial College Press: London, 2001; Chapter 4.
(24) Calabrese, G. S.; Lin, M. S.; Dresner, J.; Wrighton, M. S. *J. Am. Chem. Soc.* **1982**, *104*, 2412.
(25) Tan, M. X.; Kenyon, C. N.; Lewis, N. *J. Phys. Chem.* **1994**, *98*, 4959.
(26) Tan, M. X.; Kenyon, C. N.; Christian, W.; Wilisch, A.; Lewis, N. S. *J. Electrochem. Soc.* **1995**, *142*, L62.
(27) Gangotri, K. M.; Lal, C. *Int. J. Eng. Res.* **2000**, *24*, 365.
(28) Salvador, P. *J. Phys. Chem. B* **2001**, *105*, 6128.
(29) Hodes, G.; Howell, I. D. J.; Peter, L. M. *J. Electrochem. Soc.* **1992**, *139*, 3136−3140.
(30) Formally, we should use the term "hole" only when referring to a positively charged quasi-particle that obeys Fermi−Dirac statistics (i.e., it refers to a missing free electron in an ensemble of electrons). Still, the use of the concept is so ingrained as a synonym for any positively charged electronic charge carrier that we will follow it here, too.
(31) Kronik, L.; Ashkenasy, N.; Leibovitch, M.; Fefer, E.; Shapira, Y.; Gorer, S.; Hodes, G. *J. Electrochem. Soc.* **1998**, *145*, 1748.
(32) Sirimanne, P. M.; Shirata, T.; Damorade, L.; Hayashi, Y.; Soga, T.; Jimbo, T. *Sol. Energy Mater. Sol. Cells* **2003**, *77*, 15.
(33) Gregg, B. A.; Pichot, F.; Ferrere, S.; Fields, C. L. *J. Phys. Chem. B* **2001**, *105*, 1422.
(34) Tang, C. W. *Appl. Phys. Lett.* **1986**, *48*, 183.
(35) Ramsdale, C. M.; Barker, J. A.; Arias, A. C.; MacKenzie, J. D.; Friend, R. H.; Greenham, N. C. *J. Appl. Phys.* **2002**, *92*, 4266.
(36) Yu, G.; Gao, J.; Hummelen, J. C.; Wudl, F.; Heeger, A. J. *Science* **1995**, *270*, 1789.
(37) Shaheen, S. E.; Brabec, C. J.; Sariciftci, N. S.; Padinger, F.; Fromherz, T.; Hummelen, J. C. *Appl. Phys. Lett.* **2001**, *78*, 841−843.
(38) Brabec, C. J.; Cravino, A.; Meissner, D.; Sariciftci, N. S.; Fromherz, T.; Rispens, M. T.; Sanchez, L.; Hummelen, J. C. *Adv. Funct. Mater.* **2001**, *11*, 374−380.
(39) Huynh, W. U.; Dittmer, J. J.; Alivisatos, A. P. *Science* **2002**, *295*, 2425.
(40) McFarland, E. W.; Tang, J. *Nature* **2003**, *421*, 616.
(41) Trupke, T.; Würfel, P.; Uhlendorf, I.; Lauermann, I. *J. Phys. Chem. B* **1999**, *103*, 1905−1910.
(42) Zaban, A.; Meier, A.; Gregg, B. A. *J. Phys. Chem. B* **1997**, *101*, 7985−7990.
(43) Bisquert, J.; Garcia-Belmonte, G.; Fabregat Santiago, F. *J. Solid State Electrochem.* **1999**, *3*, 337−347.
(44) Fabregat-Santiago, F.; Mora-Seró, I.; Garcia-Belmonte, G.; Bisquert, J. *J. Phys. Chem. B* **2003**, *107*, 758−769.
(45) van de Lagemaat, J.; Park, N.-G.; Frank, A. J. *J. Phys. Chem. B* **2000**, *104*, 2044−2052.
(46) Fabregat-Santiago, F.; Garcia-Belmonte, G.; Bisquert, J.; Zaban, A.; Salvador, P. *J. Phys. Chem. B* **2002**, *106*, 334−339.
(47) Schlichthörl, G.; Huang, S. Y.; Sprague, J.; Frank, A. J. *J. Phys. Chem. B* **1997**, *101*, 8141−8155.
(48) Franco, G.; Gehring, J.; Peter, L. M.; Ponomarev, E. A.; Uhlendorf, I. *J. Phys. Chem. B* **1999**, *103*, 692−698.
(49) Abayev, I.; Zaban, A.; Fabregat-Santiago, F.; Bisquert, J. *Phys. Status Solidi A* **2003**, *196*, R4−R6.
(50) Kron, G.; Egerter, T.; Werner, J. H.; Rau, W. *J. Phys. Chem. B* **2003**, *107*, 3556.
(51) Schwarzburg, K.; Willig, F. *J. Phys. Chem. B* **2003**, *107*, 3552−3555.
(52) Oster, G.; Perelson, A.; Katchalsky, A. *Nature* **1971**, *234*, 393.
(53) Pelton, A. D. *J. Chim. Phys.* **1992**, *89*, 1931.
(54) Jamnik, J.; Maier, J. *Phys. Chem. Chem. Phys.* **2001**, *3*, 1668.
(55) Bisquert, J. *J. Phys. Chem. B* **2002**, *106*, 325−333.
(56) Lenzmann, F.; Krueger, J.; Burnside, S.; Brooks, K.; Grätzel, M.; Gal, D.; Rühle, S.; Cahen, D. *J. Phys. Chem. B* **2001**, *105*, 6347−6352.
(57) Zaban, A.; Ferrere, S.; Gregg, B. A. *J. Phys. Chem. B* **1998**, *102*, 452−460.
(58) Pichot, F.; Gregg, B. A. *J. Phys. Chem. B* **2000**, *104*, 6−10.
(59) Ferber, J.; Luther, J. *J. Phys. Chem. B* **2001**, *105*, 4895−4903.
(60) Tributsch, H. *Appl. Phys. A* **2001**, *73*, 305−316.
(61) Zhu, K.; Schiff, E. A.; Park, N. G.; van de Lagemaat, J.; Frank, A. J. *Appl. Phys. Lett.* **2001**, *80*, 685−687.
(62) Kuciauskas, D.; Freund, M. S.; Gray, H. B.; Winkler, J. R.; Lewis, N. S. *J. Phys. Chem. B* **2001**, *105*, 392−403.
(63) Haque, S. A.; Tachibana, Y.; Klug, D. R.; Durrant, J. R. *J. Phys. Chem. B* **1998**, *102*, 1745.
(64) Tachibana, Y.; Haque, S. A.; Mercer, I. P.; Durrant, J. R.; Klug, D. R. *J. Phys. Chem. B* **2000**, *104*, 1198−1205.
(65) Kelly, C. A.; Farzad, F.; Thompson, D. W.; Stipkala, J. M.; Meyer, G. J. *Langmuir* **1999**, *15*, 7047−7054.
(66) Fisher, A. C.; Peter, L. M.; Ponomarev, E. A.; Walker, A. B.; Wijayantha, K. G. U. *J. Phys. Chem. B* **2000**, *104*, 949−958.
(67) Bauer, C.; Boschloo, G.; Mukhtar, E.; Hagfeldt, A. *J. Phys. Chem. B* **2002**, *106*, 12693.
(68) Montanari, I.; Nelson, J.; Durrant, J. R. *J. Phys. Chem. B* **2002**, *106*, 12203.
(69) Zaban, A.; Greenshtein, M.; Bisquert, J. *ChemPhysChem* **2003**, *4*, 859−894.
(70) Bisquert, J.; Zaban, A.; Salvador, P. *J. Phys. Chem. B* **2002**, *106*, 8774.
(71) Nelson, J. *Phys. Rev. B* **1999**, *59*, 15374.
(72) Nelson, J.; Haque, S. A.; Klug, D. R.; Durrant, J. R. *Phys. Rev. B* **2001**, *63*, 205321-1-9.
(73) Barzykin, A. V.; Tachiya, M. *J. Phys. Chem. B* **2002**, *106*, 4356−4363.
(74) Usami, A.; Ozaki, H. *J. Phys. Chem. B* **2001**, *105*, 4577−4583.
(75) Peter, L. M.; Duffy, N. W.; Wang, R. L.; Wijayantha, K. G. U. *J. Electroanal. Chem.* **2002**, *524*−*525*, 127−136.
(76) Nusbaumer, H.; Moser, J. E.; Zakeeruddin, S. M.; Nazeeruddin, M. K.; Grätzel, M. *J. Phys. Chem. B* **2001**, *105*, 10461.
(77) Oskam, G.; Bergeron, B. V.; Meyer, G. J.; Searson, P. C. *J. Phys. Chem. B* **2001**, *105*, 6867.
(78) Hagfeldt, A.; Grätzel, M. *Acc. Chem. Res.* **2000**, *33*, 269−277.
(79) Hagfeldt, A.; Gratzel, M. *Chem. Rev.* **1995**, *95*, 49−68.
(80) Tauc, J. *Photo and Thermoelectric Effects in Semiconductors*; Pergamon: Oxford, England, 1962.
(81) Tennakone, K.; Kumara, G.; Kottegoda, I. R. M.; Perera, V. P. S. *Chem. Commun.* **1999**, 15.
(82) Tada, H.; Hattori, A. *J. Phys. Chem. B* **2000**, *104*, 4585.
(83) Bedja, I.; Kamat, P. V. *J. Phys. Chem.* **1995**, *99*, 9182.
(84) Tennakone, K.; Bandaranayake, P. K. M.; Jayaweera, P. V. V.; Konno, A.; Kumara, G. R. R. A. *Physica E* **2002**, *14*, 190.
(85) Zaban, A.; Chen, S. G.; Chappel, S.; Gregg, B. A. *Chem. Commun.* **2000**, *22*, 2231−2232.
(86) Diamant, Y.; Chen, S. G.; Melamed, O.; Zaban, A. *J. Phys. Chem. B* **2003**, *107*, 1977.
(87) Palomares, E.; Cliffort, J. N.; Haque, S. A.; Lutz, T.; Durrant, J. R. *J. Am. Chem. Soc.* **2003**, *125*, 475.
(88) Newman, J. S.; Tobias, C. W. *J. Electrochem. Soc.* **1962**, *1962*, 1183.
(89) Bisquert, J.; Garcia-Belmonte, G.; Fabregat-Santiago, F.; Ferriols, N. S.; Bogdanoff, P.; Pereira, E. C. *J. Phys. Chem. B* **2000**, *104*, 2287−2298.
(90) Stangl, R.; Ferber, J.; Luther, J. *Sol. Energy Mater. Sol. Cells* **1998**, *54*, 255−264.
(91) Papageorgiou, N.; Grätzel, M.; Infelta, P. P. *Sol. Energy Mater. Sol. Cells* **1996**, *44*, 405−438.
(92) Solbrand, A.; Lindström, H.; Rensmo, H.; Hagfeldt, A.; Lindquist, S. E.; Södergren, S. *J. Phys. Chem. B* **1997**, *101*, 2514−2518.
(93) Solbrand, A.; Henningsson, A.; Sodergren, S.; Lindstrom, H.; Hagfeldt, A.; Lindquist, S.-E. *J. Phys. Chem. B* **1999**, *103*, 1078−1083.

(94) Nakade, S.; Kambe, S.; Kitamura, T.; Wada, Y.; Yanagida, S. *J. Phys. Chem. B* **2001**, *105*, 9105−9152.
(95) Kopidakis, N.; Schiff, E. A.; Park, N.-G.; van de Lagemaat, J.; Frank, A. J. *J. Phys. Chem. B* **2000**, *104*, 3930.
(96) Hagfeldt, A.; Björstén, U.; Lindquist, S.-E. *Sol. Energy Mater. Sol. Cells* **1992**, *27*, 293.
(97) Södergren, S.; Hagfeldt, A.; Olsson, J.; Lindquist, S. E. *J. Phys. Chem. B* **1994**, *98*, 5552−5556.
(98) Peter, L. M.; Ponomarev, E. A.; Franco, G.; Shaw, N. J. *Electrochim. Acta* **1999**, *45*, 549.
(99) Huang, S. Y.; Schlichthörl, G.; Nozik, A. J.; Grätzel, M.; Frank, A. J. *J. Phys. Chem. B* **1997**, *101*, 2576−2582.
(100) Dittrich, T.; Lebedev, E. A.; Weidmann, J. *Phys. Status Solidi A* **1998**, *167*, R5−R6.
(101) Zaban, A.; Zhang, J.; Diamant, Y.; Melemed, O.; Bisquert, J. *J. Phys. Chem. B* **2003**, *107*, 6022−6025.
(102) de Jongh, P. E.; Vanmaekelbergh, D. *Phys. Rev. Lett.* **1996**, *77*, 3427−3430.
(103) Dloczik, L.; Ileperuma, O.; Lauerman, I.; Peter, L. M.; Ponomarev, E. A.; Redmond, G.; Shaw, N. J.; Uhlendorf, I. *J. Phys. Chem. B* **1997**, *101*, 10281−10289.
(104) Cao, F.; Oskam, G.; Meyer, G. J.; Searson, P. C. *J. Phys. Chem.* **1996**, *100*, 17021−17027.
(105) van de Lagemaat, J.; Frank, A. J. *J. Phys. Chem. B* **2000**, *104*, 4292−4294.
(106) Könenkamp, R. *Phys. Rev. B* **2000**, *61*, 11057.
(107) Kambili, A.; Walker, A. B.; Qiu, F. L.; Fisher, A. C.; Savin, A. D.; Peter, L. M. *Physica E* **2002**, *14*, 203−209.
(108) Bisquert, J. *J. Phys. Chem. B* **2003**, *107*, 13541−13543; *J. Phys. Chem. B* **2004**, *108*, 2323−2332.
(109) Bisquert, J.; Zaban, A. *Appl. Phys. A* **2003**, *77*, 507−514.
(110) Bisquert, J.; Vikhrenko, V. S. *J. Phys. Chem. B* **2004**, *108*, 2313−2322.
(111) Gregg, B. A. *J. Phys. Chem. B* **2003**, *107*, 4688.
(112) Only the difference between the low and high electronic energy states of the dye absorber, ($E_H - E_L$), is an observable. These energy states may be represented by the energies of the HOMO and LUMO of the absorber, which are measurable quantities, assuming that the HOMO and LUMO levels are measured for the neutral system, after relaxation. Note that μ_{low} (μ_D) and μ_{high} (μ_{D^*}) represent electron free energies (i.e., they differ from HOMO and LUMO levels (and from E_H and E_L) by the entropy of the electrons in the system).
(113) The chemical potential of the electrons in the dye molecule is equivalent to the molecule's redox potential (cf. Reiss, H. *J. Phys. Chem.* **1985**, *89*, 3783).
(114) Bube, R. H. *Photovoltaic Materials*; Imperial College Press: London, 1998.
(115) The sum of the chemical potential and the (electrostatic potential times the unit charge) equals the electrochemical potential.
(116) The electrochemical potential, η, equals $\mu - q\phi$, where q is the charge of the electron. Therefore, $\eta = \mu$ if $\phi = 0$, and $\Delta\eta = \Delta\mu$ if $\Delta\phi = 0$ (i.e., zero electric field).